Numerical analysis on cold storage characteristic of nanoparticle-enhanced phase change material for energy saving

Li Xinfang[1] Wang Xianju[2] Zhu Dongsheng[3]

([1]Zhongshan Torch Polytechnic, Zhongshan 528436, China)

([2]College of Science, South China Agriculture University, Guangzhou 510642, China)

([3]Guangzhou Institute of Energy Conversion, Chinese Academy of Sciences, Guangzhou 510640, China)

Abstract: The cold storage characteristic of nanoparticle-enhanced phase change material (NEPCM) was investigated by using numerical simulation method with Fluent software. The influence of Grashof number and particle concentration on the cold storage performance was discussed . The numerical results indicate that the cold storage characteristic of the NEPCM largely depends on the volume fraction of nanoparticles, while exhibits little sensitivity to Grashof number. As the volume fraction increases, the freezing time of the NEPCM is lowered for a given initial Grashof number. The total freezing time of the NEPCM can be lowered by 16.3% with Cu nanoparticles volume fraction is 1.0%. The reduction of the freezing time is attributed to the higher thermal conductivity of the NEPCM. At the same time, less energy per unit mass of the NEPCM is needed for freezing the NEPCM because of the lower latent heat of fusion.

Key words: nanoparticle-enhanced phase change material; cold storage; freezing time; numerical simulation

中图分类号: TB611 **文献标识码**: A **文章编号**: 1000-6516(2016)06-0054-08

纳米颗粒强化相变蓄冷特性的数值模拟

李新芳[1] 王先菊[2] 朱冬生[3]

([1] 中山火炬职业技术学院 中山 528436)

([2] 华南农业大学理学院 广州 510641)

([3] 中国科学院广州能源研究所 广州 510640)

摘 要: 采用 Fluen 软件对纳米颗粒强化相变蓄冷特性进行了数值模拟, 重点分析纳米粒子添加量和 *Gr* 数对蓄冷性能的影响, 并解释其换热机理。研究结果表明: 纳米颗粒的体积分数是影响纳米颗粒强化相变材料结冰时间的一个主要因素, 但 *Gr* 数对其结冰时间影响不大。对于一给定的 *Gr* 数, 随着纳米粒子体积分数的增加, 结冰时间减少, 纳米粒子体积分数为 1.0% 时, 纳米颗粒强化相变材

收稿日期: 2016-03-15; **修订日期**: 2016-07-07

基金项目: 广东省科技计划项目(2016A010104002)、广东省高等学校优秀青年教师培养计划项目(Yq2013197)。Funded by Science and Technology Planning Project of Guangdong Province of China (Grant No. 2016A010104002), Program for Excellent Young Teachers of Higher Education Institutions of Guangdong Province of China (Grant No. Yq2013197).

作者简介: 李新芳, 女, 37 岁, 博士、副教授。Li Xinfang, femal, 37 years old, doctor and associate professor of Zhongshan Torch Polytechnic in China.

料的结冰时间降低了 16.3%。这是由于纳米颗粒强化相变材料具有较高的导热系数。另一方面，由于纳米颗粒强化相变材料融解潜热降低，则纳米颗粒强化相变材料结冰时，每单位质量的纳米颗粒强化相变材料需要的能量较少，所以纳米颗粒强化相变材料具有较高的热释放率，在相变储能应用中具有巨大优势。

关键词：纳米颗粒强化相变材料　蓄冷　结冰时间　数值模拟

1 Introduction

Because the conventional energy sources are quickly depleted and the demand of energy is growing, more and more researchers pay attention to renewable energy sources and energy storage systems. Solid-liquid phase change provides considerable advantages such as high storage capacity and nearly isothermal behavior during the melting/freezing processes. During these years, researchers have tried to find new way to develop energy storage system. Using nano technology to enhance the heat transfer indicates great opportunity in storage system. Because the thermal conductivity of conventional heat transfer fluids is low, nanotechnology is considered to enhance thermal characteristics with substantially higher conductivities. The presence of the nanoparticles in the fluids increases appreciably the effective thermal conductivity of the fluid and consequently enhances the heat transfer characteristics. Masuda et al. [1] reported that the thermal conductivity was enhanced by dispersing ultra-fine (nanosize) particles in liquids. Soon thereafter, Choi[2] first designated the new fluids with higher thermal conductivity as "naofluids". Khanafer et al. [3] simulated heat transfer characteristic of the nanofluids in a two-dimensional enclosure for various pertinent parameters. Khodadadi et al. [4] were the first to report the improved functionality of phase change material (PCM) with nanoparticles. They found that the nanoparticle-enhanced phase change materials (NEPCM) exhibit higher thermal conductivity than the base fluids. Zhu et al. [5] simulated the thermal energy storage behavior of SiC-H_2O nanofluids in a two-dimensional enclosure. Ranjbar et al. [6] studied the solidification behavior of the NEPCM and the relevant parameters . They found the nanofluid heat transfer rate increases with the increase in the nanoparticles volume fraction. Also, it was found that the temperature gradient in the liquid is too small to cause a significant natural convection in the liquid. Thus, heat conduction is dominant in heat transfer of both solid and liquid[7-8]. In this study the freezing of the NEPCM was studied.

2 Mathematical formulation

A physical model of two-dimensional enclosure is shown in Figure 1, in which the side H is filled with nanofluid. The physical dimension of the enclosure H is chosen to be 10 mm. The horizontal walls are assumed to be adiabatic, not conductive, and impervious to mass transfer. The NEPCM in the enclosure is incompressible and the flow is laminar. The particle shape and particle size distribution are uniform, and both the nanoparticles and the base fluid are in a thermal equilibrium, which is consistent with the flow velocity The nanoparticles are assumed to have a uniform shape and size. Moreover, it is assumed that both the fluid phase and nanoparticles are in thermal equilibrium state and they flow at the same velocity. The left vertical wall is maintained at a high temperature (T_H), while the right vertical wall is kept at a low temperature (T_C). The thermophysical properties of the NEPCM are assumed to be constant except for the density variation in the buoyancy force, which is based on the Boussinesq approximation.

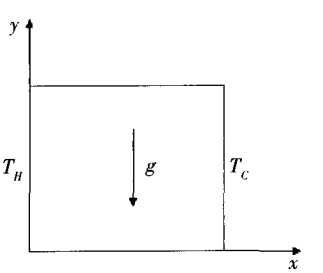

Fig. 1　Physical model of two-dimensional enclosure

Under these assumption, the governing equations are:

Continuity:

$$\frac{\partial u}{\partial x} + \frac{\partial v}{\partial y} = 0 \tag{1}$$

X-momentum equation:

$$\frac{\partial u}{\partial t} + u\frac{\partial u}{\partial x} + v\frac{\partial u}{\partial y} = \frac{1}{\rho_{nf}}\left(-\frac{\partial p}{\partial x} + \mu_{nf}\nabla^2 u + (\rho\beta)_{nf} g_x (T - T_{ref})\right) \tag{2}$$

Y-momentum equation:

$$\frac{\partial v}{\partial t} + u\frac{\partial v}{\partial x} + v\frac{\partial v}{\partial y} = \frac{1}{\rho_{nf}}\left(-\frac{\partial p}{\partial y} + \mu_{nf}\nabla^2 v + (\rho\beta)_{nf} g_y (T - T_{ref})\right) \tag{3}$$

Energy equation:

$$\frac{\partial T}{\partial t} + u\frac{\partial T}{\partial x} + v\frac{\partial T}{\partial y} = \frac{\partial}{\partial x}\left(\frac{k_{nf}}{(\rho c_p)nf}\frac{\partial T}{\partial x}\right) + \frac{\partial}{\partial y}\left(\frac{k_{nf}}{(\rho c_p)_{nf}}\frac{\partial T}{\partial y}\right) \tag{4}$$

The above equations can be cast in non-dimensional form by incorporating the following dimensionless parameters:

$$\begin{cases} X = \dfrac{x}{H} \\ Y = \dfrac{y}{H} \end{cases} \tag{5}$$

$$\begin{cases} U = \dfrac{u}{\nu/H} \\ V = \dfrac{v}{\nu/H} \end{cases} \tag{6}$$

$$\theta = \frac{T - T_L}{T_H - T_L} \tag{7}$$

The density of the NEPCM is given by:

$$\rho_{nf} = (1 - \phi)\rho_f + \phi\rho_p \tag{8}$$

Whereas the heat capacitance, latent heat of fusion for the NEPCM and part of the Boussinesq term are:

$$\rho_{nf} C_{pnf} = (1 - \phi)\rho_f C_{pf} + \phi\rho_p C_{pp} \tag{9}$$

$$\rho_{nf} L_{nf} = (1 - \phi)\rho_f L_f \tag{10}$$

$$\rho_{nf}\beta_{nf} = (1 - \phi)\rho_f\beta_f + \phi\rho_p\beta_p \tag{11}$$

With ϕ is the volume fraction of the nanoparticles and subscripts f, nf and p stand for base fluid, NEPCM and nanoparticles, respectively.

In addition, the thermal conductivity of the NEPCM was measured by a Hot Disk Thermal Constants Anlyser, and the viscosity of the NEPCM was measured using capillary viscometers.

The pertinent thermophysical properties are given in Table 1. The present processing method can be found elsewhere[3-4].

Table 1 Thermophysical properties of the nanoparticle, water and NEPCM

Property	Cu	Water	$\phi = 0.1\%$	$\phi = 1.0\%$	$\phi = 5.0\%$
ρ/(kg/m^3)	8 954	999.80	1 000.68	1 008.64	1 044.22
μ/(Pa · s)	-	1.55×10^{-3}	1.55×10^{-3}	1.60×10^{-3}	1.66×10^{-3}
c_p/(J/kg · K)	383	4 201	4 197	4 163	4 018
k/(W/m · K)	400	0.562 5	0.622 7	0.668 8	0.792
β/(1/K)	1.67×10^{-5}	7.00×10^{-5}	7.00×10^{-5}	6.95×10^{-5}	6.76×10^{-5}
L/(J/kg)	-	3.35×10^5	3.35×10^5	3.32×10^5	3.19×10^5
Pr	-	11.58	10.45	9.96	8.42

The initial and boundary conditions for the present investigation are presented as Table 2.

Table 2 Initial and boundary conditions

Initial conditions	Boundary conditions
$u = v = \dfrac{\partial T}{\partial y} = 0$	at $y = 0, H$ and $0 \leqslant x \leqslant H$
$\begin{cases} u = v = 0 \\ T = T_H \end{cases}$	at $x = 0$ and $0 \leqslant y \leqslant H$
$\begin{cases} u = v = 0 \\ T = T_C \end{cases}$	at $x = H$ and $0 \leqslant y \leqslant H$

3 Numerical methods

Starting at time $t = 0$, the temperatures of both active left and right walls were lowered by the same amount such that the cold right wall was held 10 ℃ below the freezing temperature of the base fluid ($T_H = 273.15$ and $T_C = 263.15$ K). Consequently, the NEPCM will start freezing on the right wall and the solid front travels to the left. The remaining boundary conditions were unchanged in comparison to the conditions prior to $t = 0$.

The SIMPLE method within version 6.2 of the com-

mercial code Fluent was utilized to solve the governing equations. For all the cases reported here, uniform grid spacings for both x and y directions were utilized. The calculating time step was 1s. The Quick differential algorithm was used to deal with the momentum and energy equations, whereas the PRESTO algorithm was used to deal with the pressure correction equation. The under-relaxation factors for the velocity components, pressure correction, thermal energy and liquid fraction were 0.5, 0.3, 1 and 0.9 respectively. In order to satisfy convergence criteria (10^{-7} for continuity and momentum, and 10^{-9} for thermal energy), the number of iterations for every time step was set to 1 000.

In order to verify the numerical code, comparison of the average Nusselt number along the hot wall with previous works[9-11] for different Rayleigh numbers is shown in Table 3. This table shows an excellent agreement between our results and those of other benchmark solutions, which suggests that our calculation method is adequate to describe the phase change process of the NEPCM correctly.

Table 3 Comparison of present numerical simulation with previous works

Different Rayleigh numbers	Average Nusselt number			
	Present	De Vahl Davis[9]	Barakos and Mitsoulis[10]	Fusegi et al.[11]
$Ra = 10^3$	1.122	1.118	1.114	1.105
$Ra = 10^4$	2.324	2.243	2.245	2.302
$Ra = 10^5$	4.733	4.519	4.510	4.646

4 Results and Discussion

Starting with steady natural convection within the Cu-H_2O NEPCM that is inside a differentially-heated square cavity, freezing of the Cu-H_2O NEPCM was investigated. The temperatures of the left and right walls were lowered by 10 ℃. In effect, the cold right wall was held 10℃ lower than the freezing temperature of the base fluid (273.15 K). Consequently, the NEPCM will start freezing on the right wall and the solid front travels to the left. The other boundary conditions remained unchanged. Solid particle volume fractions of 0, 0.1%, 1.0% and 5.0% were considered for two initial Grashof numbers of 10^4 and 10^5. The pertinent properties are given in Table 1. Contours of the volume fraction of the NEPCM during freezing at various time instants are shown in Figure 2 and Figure 3 for an initial Grashof number of 10^4. The time instants in Figure 2 are 100 and 600 s, the time instants in Figure 3 are 1 200 and 2 400 s. Color gray is used to identify the liquid phase, whereas color black is indicative of the frozen solid phase. In general, the sharp liquid-solid interface is nearly vertical with a mild misalignment toward the colder wall early on, thus favoring a longer wetted length on the top insulated wall. This can be attributed to the buoyancy-driven convection in the cavity that was already at full strength at $t = 0$ in the form of a clockwise (CW) rotating vortex. For $t > 0$, the strength of this vortex diminishes whereas a second counter-clockwise (CCW) rotating vortex is created next to the left wall (see Figure 4).

For this Grashof number ($Gr = 10^4$), it is observed that as the solid particle volume fraction is raised, the Cu-H_2O NEPCM will freeze more rapidly. There are two possible reasons to explain the behavior of the quicker freezing rate. One is the higher thermal conductivity for the NEPCM, because the crystal growth mainly depends on heat transfer. At the process of freezing, a large amount of heat will be discharged. If the heat can't be released in time, the freezing process will be hindered. After adding the nanoparticles to the base fluid, the fluid has higher thermal conductivity. Therefore, the freezing speed of the NEPCM is able to be accelerated. Another reason may be the Cu nanoparticles acting as a nucleating agent. It is known that the freezing process of pure water has a supercooling degree about 4 ℃. When the nanoparticles are added into water, the supercooling degree of water is decreased according to the mechanism of heterogeneous nucleation. The beginning of freezing time is ahead. This is also helpful to save the freezing time.

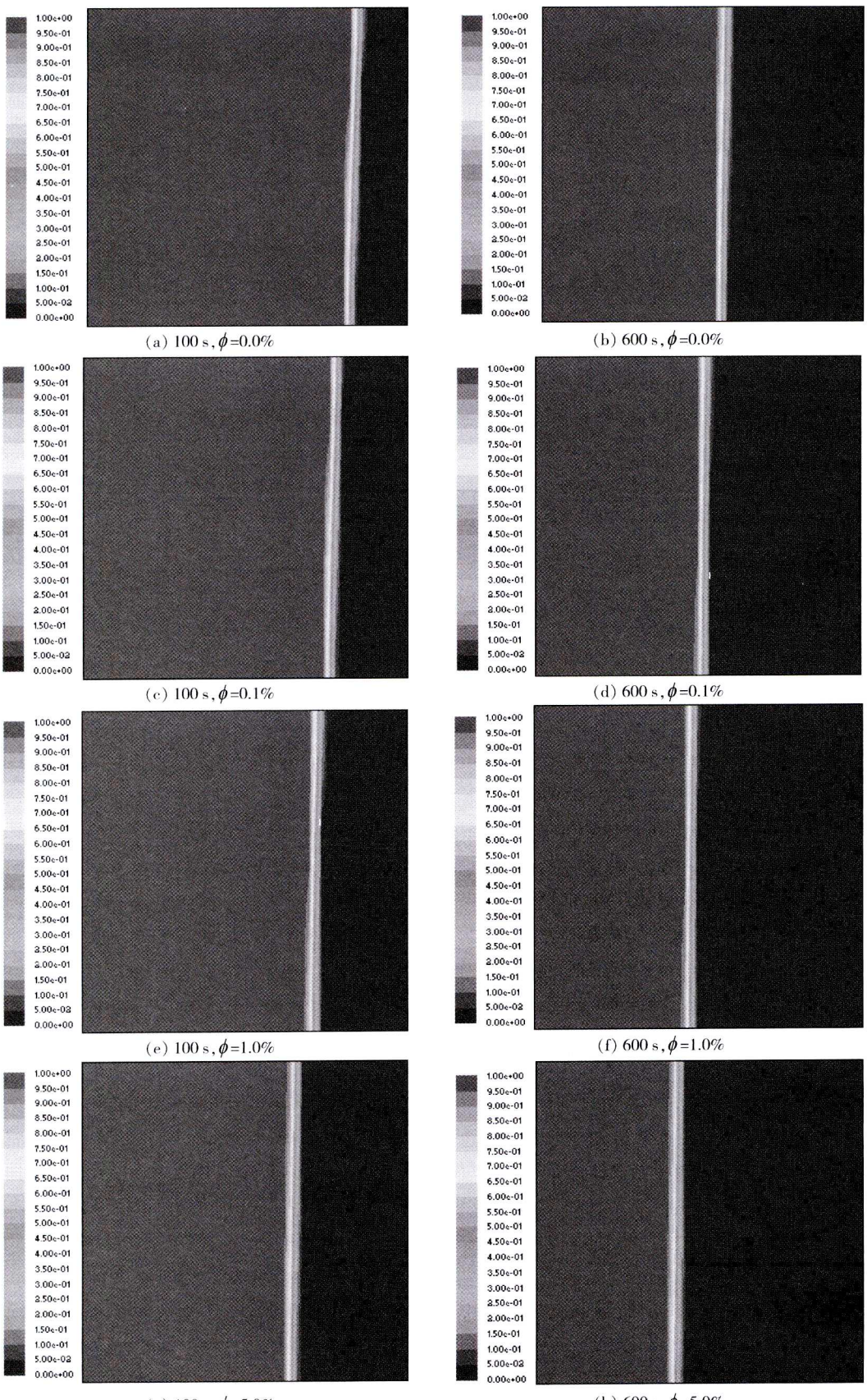

(a) 100 s, ϕ=0.0%　(b) 600 s, ϕ=0.0%

(c) 100 s, ϕ=0.1%　(d) 600 s, ϕ=0.1%

(e) 100 s, ϕ=1.0%　(f) 600 s, ϕ=1.0%

(g) 100 s, ϕ=5.0%　(h) 600 s, ϕ=5.0%

Fig. 2 Contours of volume fraction of NEPCM at various time instants during freezing course ($Gr = 10^4$)

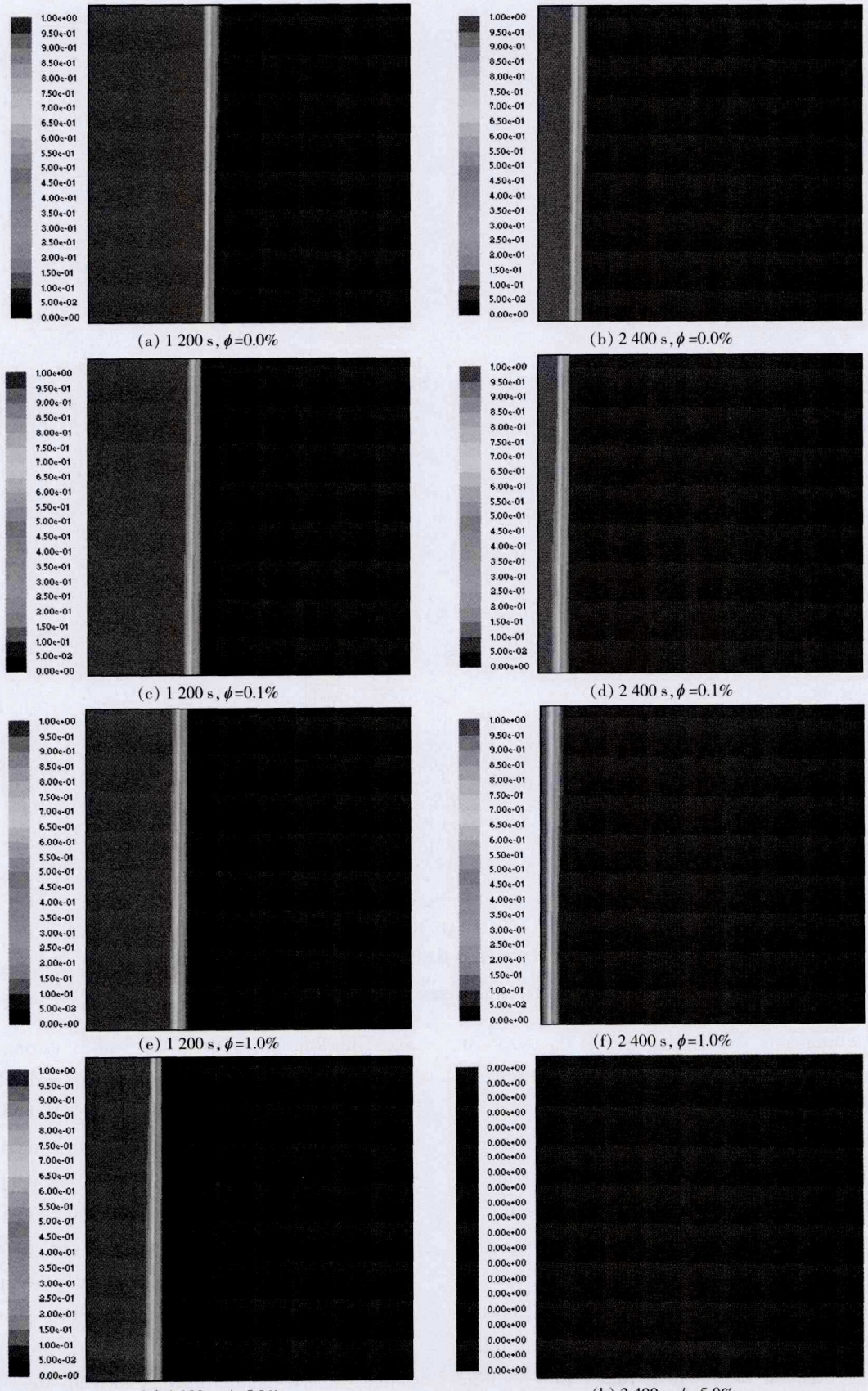

(a) 1 200 s, ϕ=0.0%　(b) 2 400 s, ϕ=0.0%

(c) 1 200 s, ϕ=0.1%　(d) 2 400 s, ϕ=0.1%

(e) 1 200 s, ϕ=1.0%　(f) 2 400 s, ϕ=1.0%

(g) 1 200 s, ϕ=5.0%　(h) 2 400 s, ϕ=5.0%

Fig. 3　Contours of volume fraction of NEPCM at various time instants during freezing course ($Gr = 10^4$)

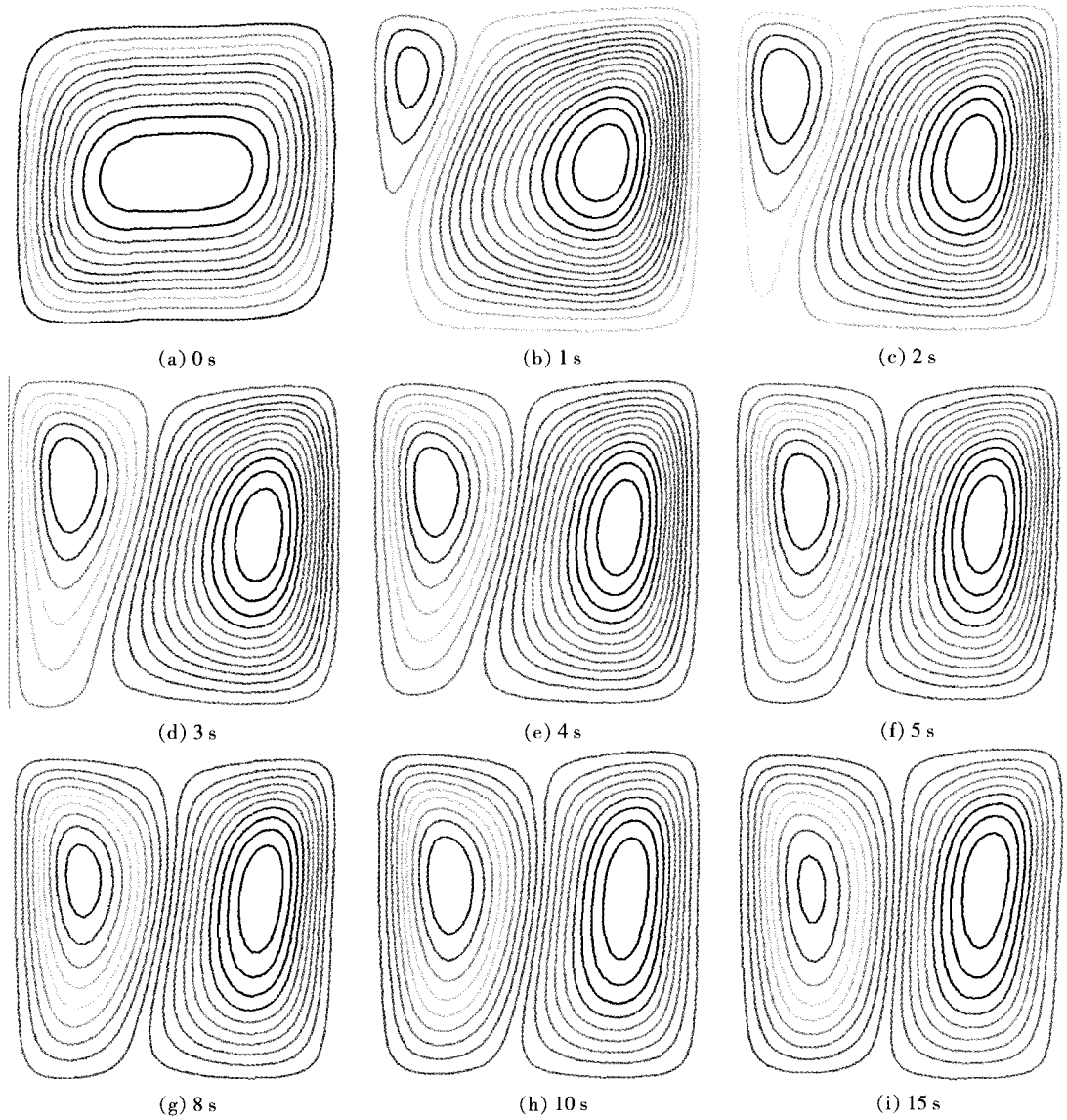

Fig. 4 Streamline patterns of Cu-H_2O NEPCM at various time instants for initial 15 s during freezing course ($Gr = 10^4$, $\phi = 1.0\%$)

The instantaneous streamlines within the NEPCM for the initial 15s during the freezing of the NEPCM for an initial $Gr = 10^4$ and a solid particle volume fraction of 1% are shown in Figure 4. The streamlines at $t = 0$ correspond to a similar case studied by Khanafer et al. [3] and Khodadadi et al[4], and a CW rotating vortex is clearly observed. As a result of the sudden lowering of the temperatures of the two active walls at $t > 0$, the CW rotating vortex diminishes in strength and spatial coverage due to formation of a CCW rotating vortex next to the left wall. The creation of the dual-vortex flow pattern was examined in greater detail by lowering the time step to 0. 1 s for this case. Note that the formation, growth and equilibration of the CCW vortex during the initial 15 s involves a dynamic interaction with the initially strong CW vortex. At the t = 10-15 s instant, two vortices rotating in opposite directions and nearly equal in size are observed squeezed between the left wall and a thin frozen layer next to the right wall. For the remainder of the freezing process, the dual-vortex structure will persist however due to the leftward movement of the freezing front, the vortices will shrink in coverage space and their strength will decay. It should be noted that the actual Grashof number for this unsteady freezing problem decreases with time due to the continuous shrinking of the distance between the left wall and the liquid-solid

interface.

The freezing times for pure water and Cu-H_2O NEPCM for initial Grashof numbers of 10^4 and 10^5 are summarized in Table 4. The liquid volume that continuously decreases from the start of the freezing exhibits little sensitivity to the value of the initial Grashof number. On the other hand, the volume of the NEPCM is strongly dependent on the solid particle volume fraction of the dispersed nanoparticles. For a given initial Grashof number($Gr = 10^4$), The whole freezing time of distilled water is 3 and 130 s, 0.1% NEPCM is 2 and 820 s, 1.0% NEPCM is 2 and 620 s, and 5.0% NEPCM is 2 and 210 s, and the whole freezing time of the three NEPCM can be lowered by 9.9%, 16.3%, and 29.4%, respectively. It reveals that the higher the nanoparticle volume fraction is, the faster the decrease of the liquid volume fraction, and the shorter the whole freezing time. The reduction of the freezing time is attributed to the higher thermal conductivity of the NEPCM. At the same time, less energy per unit mass of the NEPCM is needed for freezing the NEPCM because of the lower latent heat of fusion. This phenomenon is in agreement with the study of Liu[12], who experimentally investigated TiO_2-$BaCl_2$-H_2O suspensions for thermal energy storage, respectively. Thus, the application of NEPCM in the cooling industry can improve the performance of refrigeration systems and save the running time for refrigeration systems.

Table 4　Freezing time of Cu-H_2O NEPCM

Freezing time t	Volume fraction ϕ			
	0.0%	0.1%	1.0%	5.0%
t_1 ($Gr = 10^4$)	3 130	2 820	2 620	2 210
t_2 ($Gr = 10^5$)	3 160	2 860	2 660	2 230

5　Conclusions

In order to solve the imbalance of electrical demand in summer and save energy, using the thermal energy storage of phase change material is one of the effective ideas. The potential of Cu-H_2O NEPCM as a new PCM was investigated numerically in this study. Probably due to the enhancemant of thermal conductivity, the freezing rate of fluids is enhanced. The whole freezing time can be saved by 9.9%, 16.3%, and 29.4% at the 0.1%, 1.0%, and 5.0% NEPCM. The reasons for this phenomenon may be the higher thermal conductivity for the NEPCM and the Cu nanoparticles acting as a nucleating agent. In summary, the calculated quicker freezing rate of the NEPCM is a clear indicator of its great potential for thermal energy storage applications.

Reference

1　Masuda H, Ebata A, Hishinuma N. Alteration of Thermal Conductivity and Viscosity of Liquid by Dispersing Ultra-Fine Particles[J]. Netsu Bussei, 1993(4): 227-233.

2　Choi S U S. Enhancing Thermal conductivity of fluids with nanoparticles. In: Siginer D A, Wang H P. Developments and application of non-newtonian flows[C]. ASTM Spec. Tech. Publ., 1995: 99-105.

3　Khanafer K, Vafai K, Lightstone M L. Buoyancy-driven heat transfer enhancement in a two-dimentional enclosure utilizing nanofluids[J]. Int. J. Heat Mass Transfer, 2003, 19: 3639-3653.

4　Khodadadi J, Hosseinizadeh S F. Nanoparticle-enhanced phase change materials (NEPCM) with great potential for improved thermal energy storage[J]. Int. J. Comm Heat Mass Transfer, 2007, 34: 534-543.

5　Zhu D S, Wu S Y, Yang S. Numerical simulation on thermal energy storage behavior of SiC-H_2O nanofluids[J]. Energy Sources, Part A, 2011, 33: 1317-1325.

6　Ranjbar A A, Kashani S, Hosseinizadeh S F, et al. Numerical heat transfer studies of a latent heat storage containing nano-enhanced phase change material[J]. Thermal Science, 2011, 15: 169-181.

7　Kashani S, Ranjbar A A, Abdollahzadeh M, et al. Solidification of nano-enhanced phase change material (NEPCM) in a wavy cavity[J]. Heat and Mass Transfer, 2012, 48(7): 1155-1166.

8　Hosseini S M J, Ranjbar A A, Sedighi K, et al. Melting of nanoprticle-enhanced phase change material inside shell and tube heat exchanger [J]. Journal of Engineering, 2013: 8.

9　De Vahl Davis G, Jones I P. Natural caonvection of air in a square cavity: a comparison exercise[J]. Int J for Num Meth in Fluids, 1983, 3: 227-248.

10　Barakos G, Mitsoulis E. Natural flow in a square cavity revisited: laminar and turbulent models with wall function[J]. Int J for Num Methods in Fluids, 1994, 18(7): 695-719.

11　Fusegi T, Hyun J M K, Kuwahara B F. A numerical study of three-dimensional natural convection in a differentially heated cubical enclosure[J]. Int. J. Heat Mass Transfer, 1991, 34: 1543-1557.

12　刘玉东. 纳米复合低温相变蓄冷材料的制备及热物性研究[D]. 重庆: 重庆大学, 2005.
Liu Y D. Study on preparation and thermal properties of phase change nanocomposites for cool storage[D]. Chongqing: Chongqing University, China, 2005.